Published in final edited form as:
Gastroenterology. 2008 June ; 134(7): 2080–2090. doi:10.1053/j.gastro.2008.02.084.

Oncogenic KRAS induces progenitor cell expansion and malignant transformation in zebrafish exocrine pancreas

Seung Woo Park[1], **Jon M Davison**[2], **Jerry Rhee**[1], **Ralph H. Hruban**[2,3], **Anirban Maitra**[2,3], and **Steven D Leach**[1,3,4]

1*Department of Surgery, The Sol Goldman Center for Pancreatic Cancer Research, Johns Hopkins University School of Medicine, Baltimore, MD 21205*

2*Department of Pathology, The Sol Goldman Center for Pancreatic Cancer Research, Johns Hopkins University School of Medicine, Baltimore, MD 21205*

3*Department of Oncology, The Sol Goldman Center for Pancreatic Cancer Research, Johns Hopkins University School of Medicine, Baltimore, MD 21205*

4*Department of Cell Biology, The Sol Goldman Center for Pancreatic Cancer Research, Johns Hopkins University School of Medicine, Baltimore, MD 21205*

Abstract

Background and Aims—Although the cell of origin for pancreatic cancer remains unknown, prior studies have suggested that pancreatic neoplasia may be initiated in progenitor-like cells. In order to examine the effects of oncogene activation within the pancreatic progenitor pool, we devised a system for real-time visualization of both normal and oncogenic KRAS-expressing pancreatic progenitor cells in living zebrafish embryos.

Methods—Using BAC transgenes under the regulation of *ptf1a r*egulatory elements, we expressed either GFP alone or GFP fused to oncogenic KRAS in developing zebrafish pancreas.

Results—Following their initial specification, normal GFP-labeled pancreatic progenitor cells were observed to actively migrate away from the forming endodermal gut tube, and subsequently underwent characteristic exocrine differentiation. In contrast, pancreatic progenitor cells expressing oncogenic KRAS underwent normal specification and migration, but failed to differentiate. This block in differentiation resulted in the abnormal persistence of an undifferentiated progenitor pool, and was associated with the subsequent formation of invasive pancreatic cancer. These tumors exhibited several features in common with the human disease, including evidence of abnormal Hedgehog pathway activation.

Conclusions—These results provide a unique view of the tumor-initiating effects of oncogenic KRAS in a living vertebrate organism, and suggest that zebrafish models of pancreatic cancer may prove useful in advancing our understanding of the human disease.

Address correspondence to: Steven D. Leach, Johns Hopkins University, 720 Rutland Ave / Ross 771, Baltimore, MD 21205, phone 410.955.5765, fax 410.614.2913, stleach@jhmi.edu.

The authors report no conflicts of interest related to this work.

Introduction

In both mouse and human, exocrine pancreatic cancer appears to be initiated by oncogenic KRAS. In humans, over 90% of all pancreatic ductal adenocarcinomas show evidence of oncogenic KRAS mutations, and evaluation of pancreatic cancer precursor lesions suggests that these mutations represent an early event in pancreatic tumorigenesis [1, 2]. In mice, expression of oncogenic KRAS is sufficient to induce pancreatic intraepithelial neoplasia (PanIN), a known precursor for invasive pancreatic ductal adenocarcinoma [3–5]. With low frequency and long latency, oncogenic KRAS-induced murine PanIN's progress to invasive cancer, a process that is markedly accelerated by either activation of Hedgehog signaling [6] or inactivation of a variety of tumor suppressor genes, including *Trp53, Ink4a/Arf, Tgfbr2* or *Smad4* [4, 7–9]. These studies have led to the view that oncogenic KRAS functions as a critical initiator of pancreatic neoplasia, with additional genetic lesions required for tumor progression.

In spite of the known ability of oncogenic KRAS to initiate pancreatic neoplasia, the nature of KRAS-induced initiating events remains unknown. To facilitate *in vivo* examination of individual cells expressing oncogenic KRAS in the context of the exocrine pancreas, we have developed technology for targeted transgene expression in developing zebrafish pancreas. Utilizing this technology, we have generated a model of exocrine pancreatic cancer in zebrafish, and have further identified a block in progenitor cell differentiation as one of the earliest discernable effects of oncogenic KRAS expression in vertebrate exocrine pancreas.

Experimental Procedures

(See Supplemental Materials for detailed methods)

Generation of transgenic zebrafish

Using bacterial recombineering [10], we modified a genomic BAC (CH211-142H2) spanning the zebrafish *ptf1a* locus to generate transgene constructs *ptf1a:eGFP* and *ptf1a:eGFP-KRAS^{G12V}*. To enable real-time visualization of oncogenic KRAS expressing cells, the KRAS^{G12V} transgene was expressed as eGFP fusion protein[11]. The purified *ptf1a:eGFP* and *ptf1a:eGFP-KRAS^{G12V}* BAC transgenes were injected into single-cell stage wild-type AB embryos, which were then raised to adulthood and outcrossed to generate F1 founders.

Analysis of Tumor Incidence in Adult Fish

To generate a population of fish in which to assess the time interval to visible tumor formation, transgenic adult Tg(*ptf1a:eGFP-KRAS^{G12V}*) were outcrossed to wild-type fish and approximately 200 heterozygous embryos expressing eGFP in the expected pattern were raised. Transcutaneous eGFP expression was evaluated in a subset of the total number of fish at 1, 2, 3, 6 and 9 month time points. Fish with and without transcutaneous eGFP fluorescence were sacrificed at interval time points for histologic evaluation.

Immunolabeling and In situ hybridization

Immunofluorescent and in situ hybridization analyses were performed either on whole embryos or on 8μm cryosections as described previously [12]. Primary antibodies used for immunostaining, primers used to generate in situ probes, and methodology for multichannel fluorescent intensity analysis are described in the Supplemental Material.

Quantitative RT-PCR

Real-time, quantitative RT-PCR was performed using an ABI Prism 7700 Sequence Detector (Applied Biosystems), using the QuantiTect™ SYBR® Green PCR Kit (Qiagen). Primer sequences are listed in the Supplemental Materials.

Results

Generation of Tg(*ptf1a:eGFP*) and Tg(*ptf1a:eGFP-KRAS^{G12V}*) lines

In order to capture regulatory elements capable of targeting transgene expression to zebrafish pancreatic progenitor cells, we engineered a large genomic BAC spanning the ptf1a locus, so that *ptf1a* coding sequence was replaced with a cDNA encoding either eGFP alone or eGFP fused to oncogenic human KRAS 4B (Figure 1A, Figure 2A; Supplemental Figure S1). Using these BAC transgenes, seven independent Tg(*ptf1a:eGFP*) and six Tg(*ptf1a:eGFP-KRAS^{G12V}*) lines were established. In the absence of significant variation between lines, a single representative Tg(*ptf1a:eGFP*) line and a single representative Tg(*ptf1a:eGFP-KRAS^{G12V}*) line were selected for further analysis.

The ptf1a:eGFP transgene recapitulates wild-type ptf1a expression

Examination of living *ptf1a:eGFP* embryos revealed expression in retinal amacrine cells, hindbrain, spinal interneurons, and pancreas (Fig. 1, 2). This pattern faithfully recapitulated the previously reported pattern of endogenous ptf1a expression [12–14]. By crossing Tg (*ptf1a:eGFP*) fish with fish expressing mCherry fluorescent protein under the regulation of insulin promoter elements [15], we visualized the initial specification and migration of pancreatic progenitor cells with respect to the already formed principle islet (Fig. 1). In addition to expression in the early pancreatic progenitor pool, eGFP expression was subsequently observed to persist in differentiated acinar cells throughout adult life (see Fig 3A and Fig 6A below).

Pancreatic expression of ptf1a:eGFP-KRAS^{G12V} becomes progressively restricted

We next compared patterns of eGFP fluorescence in Tg(*ptf1a:eGFP*) and Tg(*ptf1a:eGFP-KRAS^{G12V}*) embryos. Expression of eGFP-KRAS^{G12V} in the retina, hindbrain and neural tube was highly similar to the pattern seen in Tg(*ptf1a:eGFP*) embryos (Fig. 2F–K). However, transgene expression in developing pancreas was much more heterogeneous among Tg (*ptf1a:eGFP-KRAS^{G12V}*) embryos, with approximately 50% of transgenic embryos exhibiting pancreatic expression levels which permitted serial imaging using a fluorescent stereomicroscope. Pancreatic progenitor cells expressing eGFP-KRAS^{G12V} underwent initial specification and migration in a manner identical to that observed in Tg(*ptf1a:eGFP*) embryos. However, when individual embryos were serially imaged between 48 and 96 hours post fertilization (hpf), we observed a noticeable decay in the intensity of eGFP-KRAS^{G12V} expression (compare Fig. 2H,J with I,K). By 96 hpf, eGFP-KRAS^{G12V} expression was best detected by confocal microscopy. Gradual loss of pancreatic eGFP fluorescence in the *ptf1a:eGFP-KRAS^{G12V}* lines was also associated with loss of *eGFP-KRAS^{G12V}* transcripts as assessed by whole mount in situ hybridization, even while transcripts for endogenous *ptf1a* were found to persist (Supplemental Fig. S2 and data not shown).

Exocrine differentiation is blocked in pancreatic progenitor cells expressing eGFP-KRAS^{G12V}

In order to assess the anatomic extent of pancreatic tissue in *ptf1a:eGFP-KRAS^{G12V}* transgenics, and also to evaluate the ability of *eGFP-KRAS^{G12V}*-expressing pancreatic progenitor cells to undergo normal exocrine differentiation, we performed immunofluorescent labeling for the digestive enzyme carboxypeptidase A (CPA), a marker of exocrine differentiation. When the dissected endodermal tissues of Tg(*ptf1a:eGFP*) larvae were examined by confocal imaging at 96 hpf, eGFP-positive cells almost uniformly co-expressed CPA in the apical cytoplasm, and showed well-developed apical secretory granules (Fig. 3A,C,E,G). In contrast to uniform expression of the *ptf1a:eGFP* transgene, pancreatic expression of the eGFP-KRAS^{G12V} fusion protein demonstrated a mosaic pattern characterized by the apparent random distribution of individual eGFP-positive cells and groups of cells (Fig.

3B,D,F,H). Notably, progenitor cells maintaining expression of the fluorescent eGFP-KRAS^{G12V} fusion protein showed negligible or extremely low levels of CPA expression, and none developed CPA-positive, apical secretory granules (Fig 3, D,H). In the context of mosaic expression of the eGFP-KRAS^{G12V} fusion protein, adjacent and surrounding cells of the exocrine pancreas lacking detectable eGFP-KRAS^{G12V} expression showed high levels of CPA in well-formed apical secretory granules. These data suggest that oncogenic KRAS cell autonomously inhibits the differentiation of pancreatic progenitor cells.

In order to quantify the ability of oncogenic KRAS to block pancreatic progenitor cell differentiation, we examined a series of optical sections of the pancreas from a total of 10 different embryos (n=4 for Tg(*ptf1a:eGFP-KRAS^{G12V}*) and n=6 for Tg(*ptf1a:eGFP*), and compared the fraction of eGFP positive pixels which were also positive for Cy3 following immunofluorescent staining for CPA. Similar to cell-by- cell FACS analysis, this pixel-by-pixel analysis allowed us to determine the fraction of eGFP-positive area that is also positive for CPA, providing a quantifiable estimate of exocrine differentiation among transgene-expressing cells (Fig. 3I,J). In *ptf1a:eGFP* larvae at 96hpf, the fraction of eGFP-positive pixels also positive for CPA was 16.0 ± 3.1% (mean ± SD), while the corresponding fraction in Tg (*ptf1a:eGFP-KRAS^{G12V}*) larvae was 2.4 ± 1.4% ($p<0.001$, unpaired T-test). These observations further support the conclusion that expression of oncogenic KRAS in exocrine pancreatic progenitors prevents these cells from undergoing a normal pattern of exocrine differentiation, resulting in the abnormal persistence of a *ptf1a*-positive, CPA-negative undifferentiated progenitor pool.

Targeted expression of eGFP-KRAS^{G12V} results in eGFP-positive pancreatic tumors

Widespread eGFP expression was sustained in the pancreas of Tg(*ptf1a:eGFP*) fish during all stages of development. This expression could be visualized transcutaneously in adult fish, allowing the overall anatomic distribution of the exocrine pancreas to be visualized (Fig. 4A). As previously reported [16, 17], adult zebrafish pancreas demonstrated a lobular configuration, with pancreatic parenchyma interposed between loops of intestine and other viscera (Fig. 4B).

Over 200 Tg(*ptf1a:eGFP-KRAS^{G12V}*) fish were raised to adulthood. By the time these fish reach the larval stage, transgene silencing has resulted in only small nests of eGFP-positive cells that are detectable by confocal microscopy, but too small to be recognized by transcutaneous fluorescence. However, as the fish aged, we observed the progressive onset of transcutaneous fluorescence, suggesting expansion of eGFP-KRAS expressing cells. A random subset of fish was periodically anesthetized and evaluated for abnormal patterns of transcutaneous eGFP expression suggestive of tumor formation. In addition, a total of 32 adult fish (18 with transcutaneous eGFP fluorescence patterns suggesting tumor formation and 14 fish without transcutaneous eGFP fluorescence) were sacrificed at different ages for detailed histologic evaluation.. At 1 month and 2 months of age, no transcutaneous fluorescence was detected among 30 adult Tg(*ptf1a:eGFP-KRAS^{G12V}*) fish, consistent with widespread transgene silencing observed in developing *ptf1a:eGFP-KRAS^{G12V}* embryos. Corresponding to this absence of detectable fluorescence, 2 month old Tg(*ptf1a:eGFP-KRAS^{G12V}*) fish had histologically normal pancreas and no evidence of tumor formation in any organ. Transcutaneous abdominal eGFP fluorescence became detectable in a fraction of Tg (*ptf1a:eGFP-KRAS^{G12V}*) fish at 3 months of age, at which time 20% of examined fish had focal areas of abdominal eGFP expression (Fig. 4C,I). The proportion of fish with transcutaneously-detectable eGFP-positive lesions increased with advancing age (Fig. 4I). At 6 months of age, 32% of fish had small (<8mm), focal eGFP-positive lesions, while 10% showed larger (>8mm) or more diffuse/multifocal areas of eGFP fluorescence. By nine months of age, two-thirds of examined fish had detectable tumor, and almost half had widespread abdominal eGFP expression characterized by either multiple, discrete foci of eGFP expression

or large masses encompassing a significant portion of the abdomen (Fig. 4D,F). Detailed histologic examination of eighteen fish with either focal or diffuse abdominal eGFP expression invariably revealed the presence of a pancreatic tumor (Fig 4G, H), and tumors associated with widespread abdominal eGFP expression exhibited overt features of malignancy (discussed in detail below). Among fourteen Tg(*ptf1a:eGFP-KRAS*^{G12V}) fish lacking transcutaneously detectable eGFP fluorescence that were subjected to histologic analysis, one showed a small tumor measuring less than 1mm in diameter, and one showed abnormal acinar cell hyperplasia (Supplemental Table S1).

Phenotypic Characteristics of Pancreatic Tumors

Histologically normal exocrine pancreas from Tg(*ptf1a:eGFP*) fish is characterized by delicately arborized clusters of pancreatic acini surrounded by adipose tissue, anatomically insinuated among loops of bowel and surrounded by other visceral organs such as the liver, spleen and gonads (Fig. 5A,B). Islet and ductal elements are also discernable (Fig. 5C). Histologic examination of abdominal eGFP-positive lesions in Tg(*ptf1a:eGFP-KRAS*^{G12V}) fish revealed tumor in each case (Table 1). Focal eGFP-positive lesions corresponded to small pancreatic tumors comprised of disorganized proliferations of cells with recognizable acinar morphology (Fig. 4G; Fig. 5E, 5F). Several fish with focal eGFP-positive tumors also showed acinar cell “hyperplasia” characterized by well-organized, but abnormally abundant acinar tissue (Fig. 5D). This feature was reminiscent of the enlarged but histologically normal pancreas previously observed prior to pancreatic tumor formation in mice [3].

When examined histologically, all fish with large, widespread abdominal eGFP-positive tumors showed defining features of malignancy: invasion of the pancreas and surrounding organs and/or evidence of apparent metastasis (summarized in Table 1). These tumors displayed considerable heterogeneity with respect to histologic patterns of differentiation, and included acinar cell carcinoma, ductal adenocarcinoma, adenocarcinomas with mixed acinar and ductal features, and mucinous (colloid) adenocarcinoma (FIG. 5E–L and Table 1). Among nineteen tumors subjected to detailed histologic analysis, nine were classified as displaying acinar or predominantly acinar differentiation (47%), five were classified as ductal or predominantly ductal (26%), and five were classifed as mixed without acinar or ductal predominance (26%). Tumors with predominantly ductal differentiation also displayed dramatic stromal expansion, similar to that observed in human pancreatic cancer (Fig. 5G, Fig. S3). Tumors were frequently observed to invade adjacent gut, liver and ovary, and were often associated with considerable tissue destruction (Fig. 5M–P). Four examined fish had discrete tumor nodules in the ovary and one fish was found to have tumor foci in a spinal vertebra and adjacent spinal cord, suggesting possible hematogenous dissemination of tumor cells (Supplemental Fig. S4). As in the case of primary tumors, metastatic lesions continued to exhibit strong GFP fluorescence.

Morphologic assessment of tumor differentiation was confirmed by additional staining for markers of acinar and ductal differentiation. In tumors with ductal features, invasive glandular structures expressed cytokeratin 18 and contained intracytoplasmic mucin, as revealed by immunofluorescent labeling and mucicarmine staining (Fig. 6A–D). To evaluate areas of apparent acinar differentiation, additional immunohistochemistry was performed using the acinar cell-specific markers, amylase and CPA (Fig. 6E–H). Acinar-like elements from eGFP-KRAS^{G12V}-induced pancreatic tumors showed only low level or focal labeling, indicating a significant degree of dedifferentiation. Histologic findings are summarized in Table 1.

In order to determine the status of downstream signaling pathways known to be activated by oncogenic KRAS, we assessed levels of phospho-AKT and phospho-ERK using immunohistochemistry (Fig. 7). In contrast to infrequent ERK and AKT phosphorylation in normal zebrafish pancreas, eGFP-KRAS^{G12V}-induced pancreatic tumors exhibited widespread

labeling for both phospho-ERK and phospho-AKT (Fig. 7A–D). Associated with activation of these pathways, tumor cells expressing oncogenic KRAS fusion protein also demonstrated an increased mitotic rate, as assessed by immunofluorescent staining for phospho-histone H3 (Fig. 7E–G).

Zebrafish Pancreatic Carcinomas Show Evidence of Active Hedgehog Signaling

Ligand-dependent activation of the hedgehog signaling pathway has been observed in invasive human pancreatic cancer as well as in PanIN lesions, and forced hedgehog activation accelerates progression of KRAS-induced tumors in mice [6, 21–23]. We therefore evaluated tumors for evidence of hedgehog pathway activation, using immunohistochemistry, in situ hybridization and quantitative RT-PCR to assess expression of hedgehog pathway components (Figure 8). These experiments revealed upregulated expression of *shh*, *dhh*, *ihha*, *ihhb*, *ptc1*, *gli1* and *smo* at the RNA level (Fig. 8G–K), and Ptc2 at the protein level (Fig. 8C and D), in tumor epithelium compared to normal epithelium from *ptf1a:eGFP* transgenics. Among these upregulated markers, *ptc1* and *gli1* represent known hedgehog target genes, thereby representing surrogate markers of hedgehog pathway activation. These findings suggest that, similar to the human disease, zebrafish pancreatic cancer is also characterized by activation of hedgehog signaling.

Discussion

The successful modeling of human disease in experimental organisms often generates unique insights with respect to initiating molecular and cellular events, and also provides a novel platform for preclinical studies of early detection, chemoprevention and treatment. In the current study, we have taken advantage of BAC recombineering technology to target fluorescent transgene expression to *ptf1a*-expressing pancreatic progenitor cells, allowing us to image the earliest events in zebrafish pancreas development, and to create a novel model of zebrafish pancreatic cancer. In addition to providing new insights regarding the influence of KRAS on the differentiation of pancreatic progenitor cells, these results also provide an important proof-of-principle regarding the ability to generate pancreatic cancer in the zebrafish species, and set the stage for future identification of genetic and small molecule modifiers of pancreatic cancer initiation and progression.

As an example of the utility the zebrafish system, our studies have revealed a block in progenitor differentiation and the attendant accumulation of undifferentiated progenitors as the earliest discernable effects of oncogenic KRAS expression in vertebrate exocrine pancreas. While the effects of oncogenic Ras proteins on cellular differentiation have frequently been examined in the context of mammalian tissue culture [18], previous *in vivo* studies have typically been limited by an inability to examine defined progenitor populations. However, a similar blockade in progenitor cell differentiation has recently been reported following expression of oncogenic KRAS in either hematopoietic or bronchoaveolar stem cells [19, 20]. In both of these settings, inhibition of differentiation was associated with expansion of an undifferentiated progenitor pool, similar to the expansion of *ptf1a*-positive, CPA-negative cells observed in our Tg (*ptf1a:eGFP-KRAS*^{G12V}) embryos.

EGFP-KRAS^{G12V}-induced zebrafish pancreatic cancers displayed specific similarities and differences with respect to mouse and human pancreatic cancer. Similar to the aggressive behavior of human pancreatic cancer, zebrafish pancreatic cancers were highly invasive, and also demonstrated a propensity for apparent metastatic spread. Also similar to human pancreatic cancer, many zebrafish tumors displayed areas of mucinous metaplasia and the classical appearance of pancreatic ductal adenocarcinoma. In addition, the observed upregulation of hedgehog pathway components suggests additional analogy between human, mouse and zebrafish pancreatic cancer [3, 21–23]. Unlike most human pancreatic cancer,

however, we frequently observed features of non-ductal differentiation, especially in early lesions. Further study will be required to determine what additional genetic and epigenetic changes may occur in both ductal and non-ductal tumors, and to what degree these genetic changes are required to support widespread expression of EGFP-KRAS^{G12V}.

The Tg(*ptf1a:eGFP-KRAS*^{G12V}) transgenic model of pancreatic cancer adds to a growing list of zebrafish tumor models, including transgenic models of T- and B-cell leukemia [24–26], pancreatic endocrine neoplasms [27], and melanoma [28]. These zebrafish cancer models provide a unique opportunity for studying interactions between known oncogenes and tumor suppressor genes [28], or between genetic lesions and environmental carcinogens [29]. In addition, these models also provide novel platforms with which to conduct high throughput screens for both genetic and small molecule modifiers of tumor progression [30]. In addition to providing novel insights regarding initiating events in pancreatic tumorigenesis, the current zebrafish model will enable these approaches to be applied to the study of pancreatic cancer.

Supplementary Material

Refer to Web version on PubMed Central for supplementary material.

Acknowledgements

We thank Dr. Yoel Kloog for kindly providing us with the pGFP-KRAS^{G12V} plasmid. This work was supported by NIH grants DK61215 and DK56211, and by a grant from the Lustgarten Foundation for Pancreatic Cancer Research. S.D.L. is also supported by the Paul K. Neumann Professorship at Johns Hopkins University.

References

1. Hruban RH, van Mansfeld AD, Offerhaus GJ, van Weering DH, Allison DC, Goodman SN, Kensler TW, Bose KK, Cameron JL, Bos JL. K-ras oncogene activation in adenocarcinoma of the human pancreas. A study of 82 carcinomas using a combination of mutant-enriched polymerase chain reaction analysis and allele-specific oligonucleotide hybridization. Am J Pathol 1993;143:545–554. [PubMed: 8342602]
2. Hruban RH, Wilentz RE, Kern SE. Genetic progression in the pancreatic ducts. Am J Pathol 2000;156:1821–1825. [PubMed: 10854204]
3. Hingorani SR, Petricoin EF, Maitra A, Rajapakse V, King C, Jacobetz MA, Ross S, Conrads TP, Veenstra TD, Hitt BA, Kawaguchi Y, Johann D, Liotta LA, Crawford HC, Putt ME, Jacks T, Wright CV, Hruban RH, Lowy AM, Tuveson DA. Preinvasive and invasive ductal pancreatic cancer and its early detection in the mouse. Cancer Cell 2003;4:437–450. [PubMed: 14706336]
4. Aguirre AJ, Bardeesy N, Sinha M, Lopez L, Tuveson DA, Horner J, Redston MS, DePinho RA. Activated Kras and Ink4a/Arf deficiency cooperate to produce metastatic pancreatic ductal adenocarcinoma. Genes Dev 2003;17:3112–3126. [PubMed: 14681207]
5. Hruban RH, Adsay NV, Albores-Saavedra J, Anver MR, Biankin AV, Boivin GP, Furth EE, Furukawa T, Klein A, Klimstra DS, Kloppel G, Lauwers GY, Longnecker DS, Luttges J, Maitra A, Offerhaus GJ, Perez-Gallego L, Redston M, Tuveson DA. Pathology of genetically engineered mouse models of pancreatic exocrine cancer: consensus report and recommendations. Cancer Res 2006;66:95–106. [PubMed: 16397221]
6. Pasca di Magliano M, Sekine S, Ermilov A, Ferris J, Dlugosz AA, Hebrok M. Hedgehog/Ras interactions regulate early stages of pancreatic cancer. Genes Dev 2006;20:3161–3173. [PubMed: 17114586]
7. Ijichi H, Chytil A, Gorska AE, Aakre ME, Fujitani Y, Fujitani S, Wright CV, Moses HL. Aggressive pancreatic ductal adenocarcinoma in mice caused by pancreas-specific blockade of transforming growth factor-beta signaling in cooperation with active Kras expression. Genes Dev 2006;20:3147–3160. [PubMed: 17114585]
8. Hingorani SR, Wang L, Multani AS, Combs C, Deramaudt TB, Hruban RH, Rustgi AK, Chang S, Tuveson DA. Trp53R172H and KrasG12D cooperate to promote chromosomal instability and widely

metastatic pancreatic ductal adenocarcinoma in mice. Cancer Cell 2005;7:469–483. [PubMed: 15894267]

9. Bardeesy N, Cheng KH, Berger JH, Chu GC, Pahler J, Olson P, Hezel AF, Horner J, Lauwers GY, Hanahan D, DePinho RA. Smad4 is dispensable for normal pancreas development yet critical in progression and tumor biology of pancreas cancer. Genes Dev 2006;20:3130–3146. [PubMed: 17114584]
10. Cotta-de-Almeida V, Schonhoff S, Shibata T, Leiter A, Snapper SB. A new method for rapidly generating gene-targeting vectors by engineering BACs through homologous recombination in bacteria. Genome Res 2003;13:2190–2194. [PubMed: 12915491]
11. Niv H, Gutman O, Henis YI, Kloog Y. Membrane interactions of a constitutively active GFP-Ki-Ras 4B and their role in signaling. Evidence from lateral mobility studies. J Biol Chem 1999;274:1606–1613. [PubMed: 9880539]
12. Lin JW, Biankin AV, Horb ME, Ghosh B, Prasad NB, Yee NS, Pack MA, Leach SD. Differential requirement for ptf1a in endocrine and exocrine lineages of developing zebrafish pancreas. Dev Biol 2004;270:474–486. [PubMed: 15183727]
13. Esni F, Ghosh B, Biankin AV, Lin JW, Albert MA, Yu X, MacDonald RJ, Civin CI, Real FX, Pack MA, Ball DW, Leach SD. Notch inhibits Ptf1 function and acinar cell differentiation in developing mouse and zebrafish pancreas. Development 2004;131:4213–4224. [PubMed: 15280211]
14. Zecchin E, Mavropoulos A, Devos N, Filippi A, Tiso N, Meyer D, Peers B, Bortolussi M, Argenton F. Evolutionary conserved role of ptf1a in the specification of exocrine pancreatic fates. Dev Biol 2004;268:174–184. [PubMed: 15031114]
15. Pisharath H, Rhee JM, Swanson MA, Leach SD, Parsons MJ. Targeted ablation of beta cells in the embryonic zebrafish pancreas using E. coli nitroreductase. Mech Dev 2007;124:218–229. [PubMed: 17223324]
16. Chen S, Li C, Yuan G, Xie F. Anatomical and histological observation on the pancreas in adult zebrafish. Pancreas 2007;34:120–125. [PubMed: 17198193]
17. Yee NS, Lorent K, Pack M. Exocrine pancreas development in zebrafish. Dev Biol 2005;284:84–101. [PubMed: 15963491]
18. Crespo P, Leon J. Ras proteins in the control of the cell cycle and cell differentiation. Cell Mol Life Sci 2000;57:1613–1636. [PubMed: 11092455]
19. Kim CF, Jackson EL, Woolfenden AE, Lawrence S, Babar I, Vogel S, Crowley D, Bronson RT, Jacks T. Identification of bronchioalveolar stem cells in normal lung and lung cancer. Cell 2005;121:823–835. [PubMed: 15960971]
20. Braun BS, Archard JA, Van Ziffle JA, Tuveson DA, Jacks TE, Shannon K. Somatic activation of a conditional KrasG12D allele causes ineffective erythropoiesis in vivo. Blood 2006;108:2041–2044. [PubMed: 16720837]
21. Berman DM, Karhadkar SS, Maitra A, Montes De Oca R, Gerstenblith MR, Briggs K, Parker AR, Shimada Y, Eshleman JR, Watkins DN, Beachy PA. Widespread requirement for Hedgehog ligand stimulation in growth of digestive tract tumours. Nature 2003;425:846–851. [PubMed: 14520411]
22. Thayer SP, Di Magliano MP, Heiser PW, Nielsen CM, Roberts DJ, Lauwers GY, Qi YP, Gysin S, Castillo CF, Yajnik V, Antoniu B, McMahon M, Warshaw AL, Hebrok M. Hedgehog is an early and late mediator of pancreatic cancer tumorigenesis. Nature. 2003
23. Prasad NB, Biankin AV, Fukushima N, Maitra A, Dhara S, Elkahloun AG, Hruban RH, Goggins M, Leach SD. Gene expression profiles in pancreatic intraepithelial neoplasia reflect the effects of Hedgehog signaling on pancreatic ductal epithelial cells. Cancer Res 2005;65:1619–1626. [PubMed: 15753353]
24. Langenau DM, Feng H, Berghmans S, Kanki JP, Kutok JL, Look AT. Cre/lox-regulated transgenic zebrafish model with conditional myc-induced T cell acute lymphoblastic leukemia. Proc Natl Acad Sci U S A 2005;102:6068–6073. [PubMed: 15827121]
25. Sabaawy HE, Azuma M, Embree LJ, Tsai HJ, Starost MF, Hickstein DD. TEL-AML1 transgenic zebrafish model of precursor B cell acute lymphoblastic leukemia. Proc Natl Acad Sci U S A 2006;103:15166–15171. [PubMed: 17015828]

26. Langenau DM, Traver D, Ferrando AA, Kutok JL, Aster JC, Kanki JP, Lin S, Prochownik E, Trede NS, Zon LI, Look AT. Myc-induced T cell leukemia in transgenic zebrafish. Science 2003;299:887–890. [PubMed: 12574629]

27. Yang HW, Kutok JL, Lee NH, Piao HY, Fletcher CD, Kanki JP, Look AT. Targeted expression of human MYCN selectively causes pancreatic neuroendocrine tumors in transgenic zebrafish. Cancer Res 2004;64:7256–7262. [PubMed: 15492244]

28. Patton EE, Widlund HR, Kutok JL, Kopani KR, Amatruda JF, Murphey RD, Berghmans S, Mayhall EA, Traver D, Fletcher CD, Aster JC, Granter SR, Look AT, Lee C, Fisher DE, Zon LI. BRAF mutations are sufficient to promote nevi formation and cooperate with p53 in the genesis of melanoma. Curr Biol 2005;15:249–254. [PubMed: 15694309]

29. Haramis AP, Hurlstone A, van der Velden Y, Begthel H, van den Born M, Offerhaus GJ, Clevers HC. Adenomatous polyposis coli-deficient zebrafish are susceptible to digestive tract neoplasia. EMBO Rep 2006;7:444–449. [PubMed: 16439994]

30. Stern HM, Zon LI. Cancer genetics and drug discovery in the zebrafish. Nat Rev Cancer 2003;3:533–539. [PubMed: 12835673]

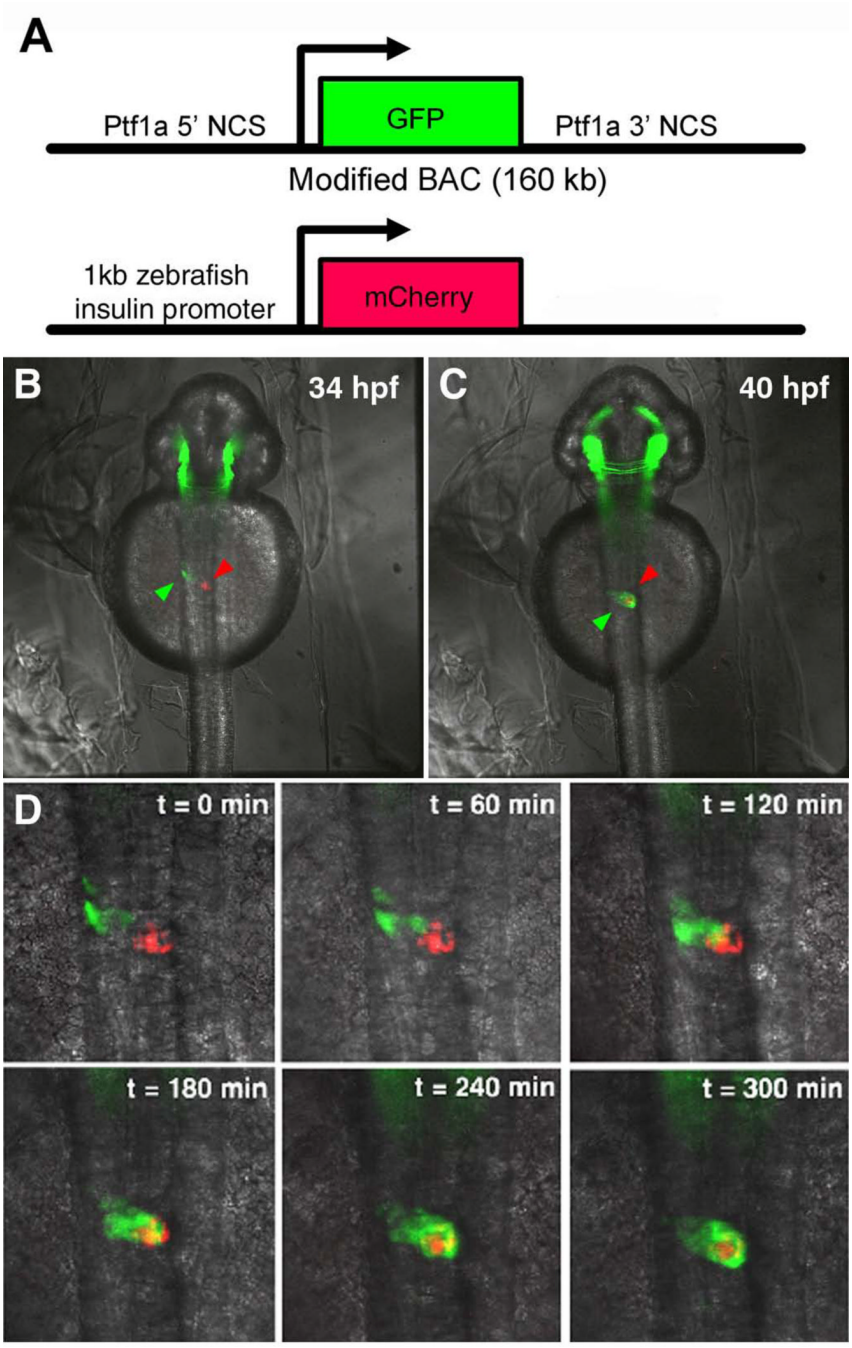

Fig. 1. Visualization of pancreatic morphogenesis in living zebrafish embryos

A, Schematic depiction of utilized transgenes. B, Merged bright and dark field images of living Tg(*ptf1a:eGFP*);(*insulin:mCherry*) double transgenic embryo at 34 hpf, demonstrating early ptf1a-expressing pancreatic progenitor cells in left lateral endoderm (green arrow), and principle islet located just to the right of the embryonic midline (red arrow). C, same embryo at 40 hpf, demonstrating migration of ptf1a-expressing progenitor cells across the midline, where they become affiliated with principle islet. D, time lapse imaging of pancreatic progenitor migration.

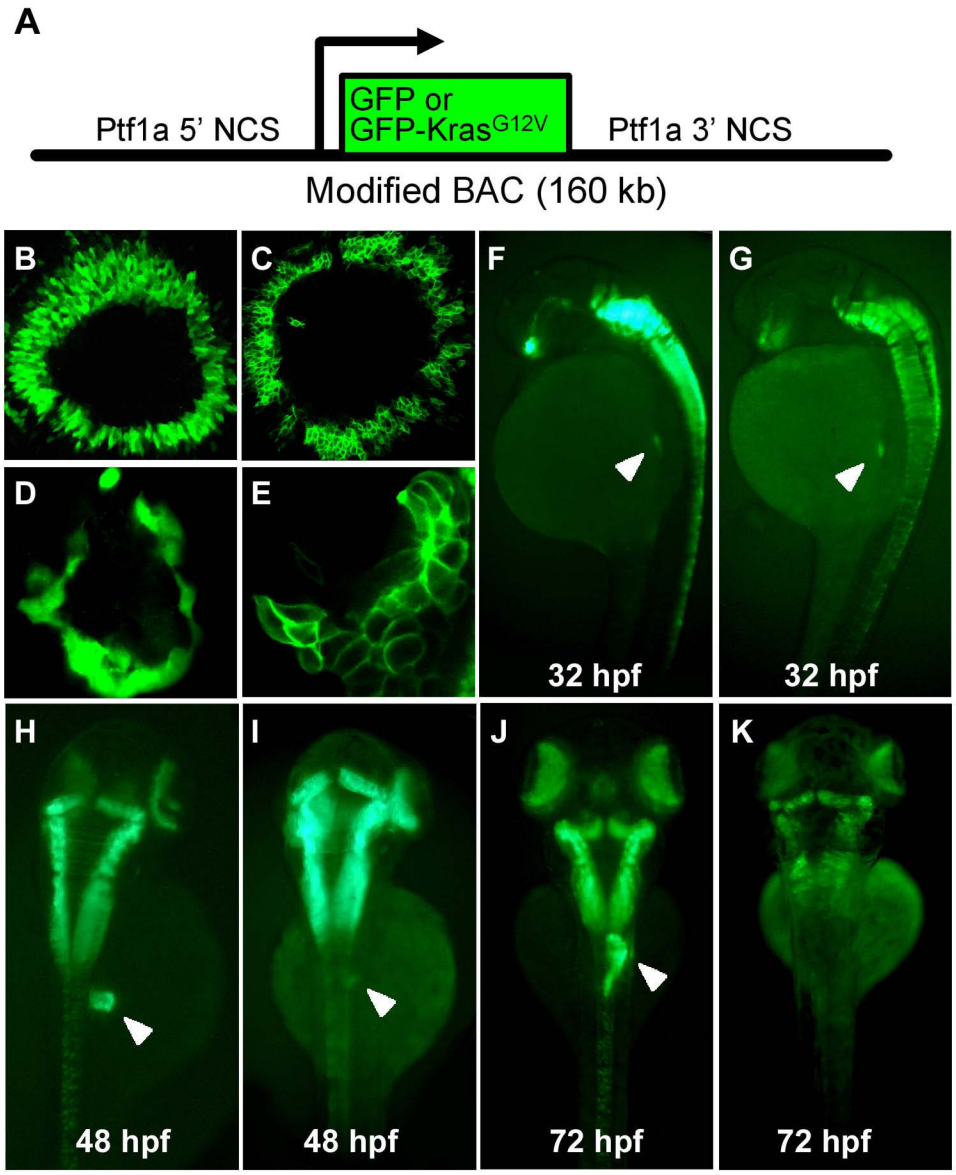

Fig. 2. Comparison of *ptf1a:eGFP* and *ptf1a:GFP-KRAS^{G12V}* transgene expression in living zebrafish embryos

A, Schematic depiction of utilized transgenes, in which *ptf1a* coding sequence was replaced with either *eGFP* or *eGFP-KRAS^{G12V}* coding sequence. B–E, Confocal images of retina (B and C) and pancreas (D and E) at 48 hpf. Note nuclear and cytoplasmic localization of eGFP in Tg(ptf1a:eGFP) embryos (B and D), compared to membrane localization of eGFP-KRAS^{G12V} fusion protein (C and E), reflecting activity of KRAS C-terminal CAAX motif. F–K, Whole mount dark field images of transgenic embryos, showing spatiotemporal expression pattern of eGFP vs. eGFP-KRAS^{G12V}. F, H, and J. *ptf1a:eGFP* embryos. G, I, and K, *ptf1a:eGFP-KRAS^{G12V}* embryos. eGFP-KRAS^{G12V}-expressing cells undergo normal specification and initial migration, but eGFP-KRAS^{G12V} is subsequently downregulated beginning at 48 hpf. White arrowheads indicate pancreatic domains of eGFP/ eGFP-KRAS^{G12V} expression.

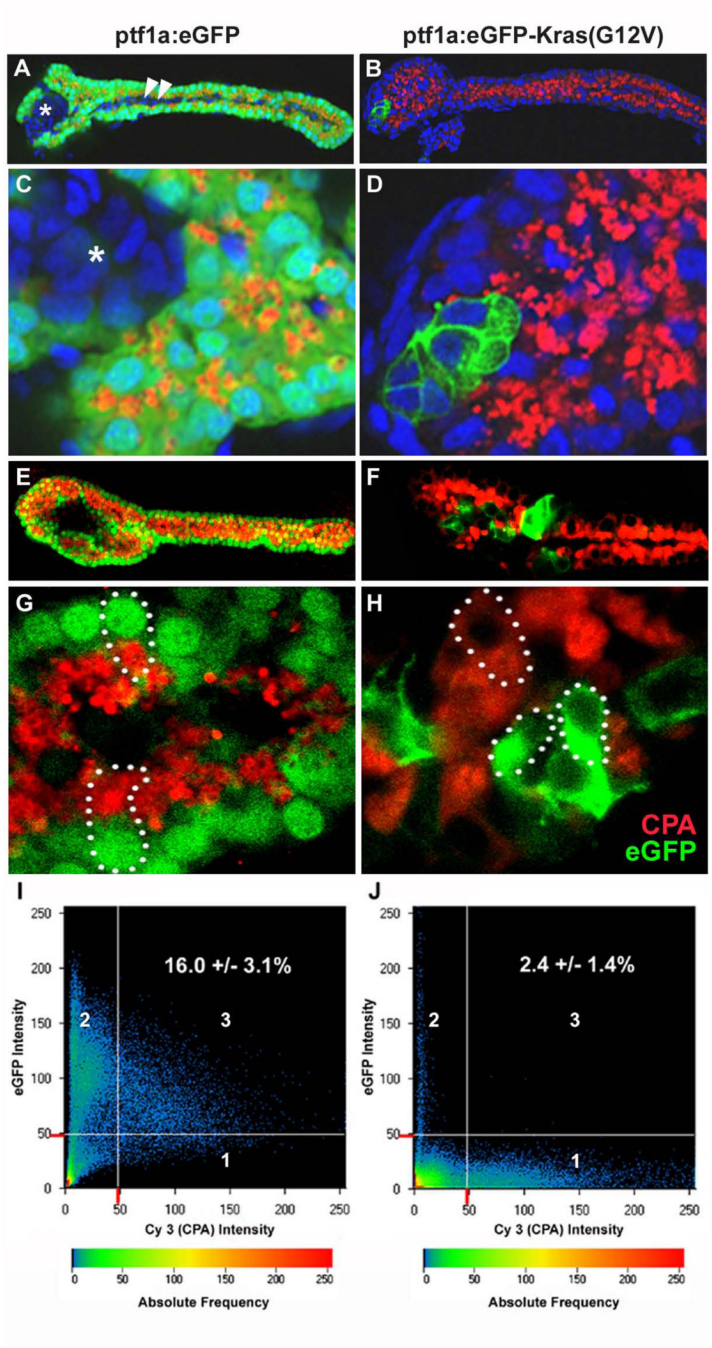

Fig. 3. Pancreatic progenitor cells with persistent eGFP-KRAS^{G12V} expression fail to undergo normal differentiation

A–H, Merged confocal images of microdissected pancreas from Tg(*ptf1a:eGFP*) and Tg (*ptf1a:eGFP-KRAS*^{G12V}) larvae at 96 hpf. Green indicates eGFP or eGFP-KRAS^{G12V} transgene expression, red Cy3 indicates immunofluorescent detection of carboxypeptidase A (CPA), a marker of exocrine differentiation. Specimens in A–D were additionally labeled with Hoechst dye. A and C, E and G represent low and high magnification images of Tg (*ptf1a:eGFP*) pancreas. B and D, F and H represent low and high magnification images of Tg (*ptf1a:eGFP-KRAS*^{G12V}) pancreas. In ptf1a:eGFP transgenic pancreas, virtually all eGFP-expressing have undergone exocrine differentiation, indicated by accumulation of CPA protein

in apical zymogen granules. In *ptf1a:eGFP-KRAS^{G12V}*- transgenic pancreas, the majority of cells do not express the transgene, and are also positive for CPA, indicating normal differentiation. In contrast, small clusters of cells with persistent eGFP-KRAS^{G12V} expression are negative for CPA, indicating failure to undergo normal differentiation. Asterisks in A and C indicate ptf1a:eGFP-negative principle islet. White arrowheads in A indicate eGFP-negative pancreatic duct. For clarity, white dots outline individual cells in G, H. I and J, Pixel-by-pixel determination of eGFP (y-axis) and CPA (x-axis) fluorescent intensity, allowing quantification of eGFP/GFP-KRAS-^{G12V} and CPA co-expression as a marker of exocrine differentiation among transgene expressing cells. Area 2 comprises eGFP-positive pixels negative for CPA, while area 3 comprises eGFP-positive pixels also positive for CPA. Area 1 comprises CPA-positive pixels negative for GFP. The percentage of all eGFP-positive pixels labeling for CPA in *ptf1a:GFP* transgenic pancreas (panel I; n=6) is 16.0 ± 3.1% (mean ± SD), compared to 2.4 ± 1.4% in *ptf1a:GFP-KRAS^{G12V}* transgenics (panel J; n=4; $p<0.001$, unpaired T-test).

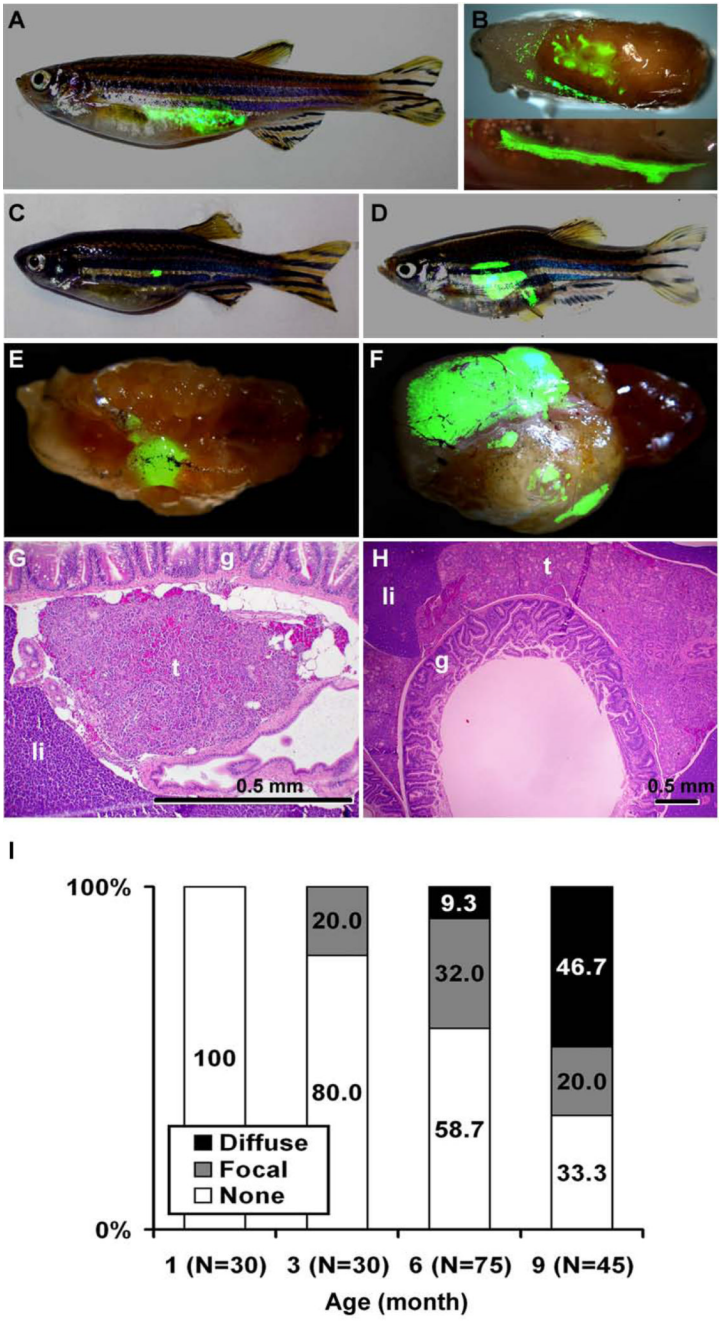

Fig. 4. Pancreatic tumor formation in adult Tg(*ptf1a:GFP-KRAS*^{G12V}) fish visualized by transcutaneous eGFP fluorescence

A, transcutaneous eGFP fluorescence in Tg(*ptf1a:eGFP*) fish, showing normal exocrine pancreas. B, low and high power image of dissected abdominal viscera from Tg (*ptf1a:eGFP*) fish, demonstrating multilobed pancreas interspersed between gut and other visceral organs. C–F. Transcutaneous (C,D) and visceral (E,F) fluorescence in Tg(*ptf1a:GFP-KRAS*^{G12V}) fish reveals eGFP-positive pancreatic tumors. Fish are designated as having either focal (C,E) or diffuse (D,F) fluorescence depending on tumor volume. G and H, histologic correlates of focal (G) and diffuse (H) transcutaneous eGFP fluorescence, confirming pancreatic tumors (note change in scale between G and H). I, proportion of randomly sampled

Tg(*ptf1a:GFP-KRAS*^{G12V}) fish with detectable fluorescent tumors, demonstrating age-associated increase in tumor incidence and extent. Abbreviations: g, gut; t, tumor; li, liver.

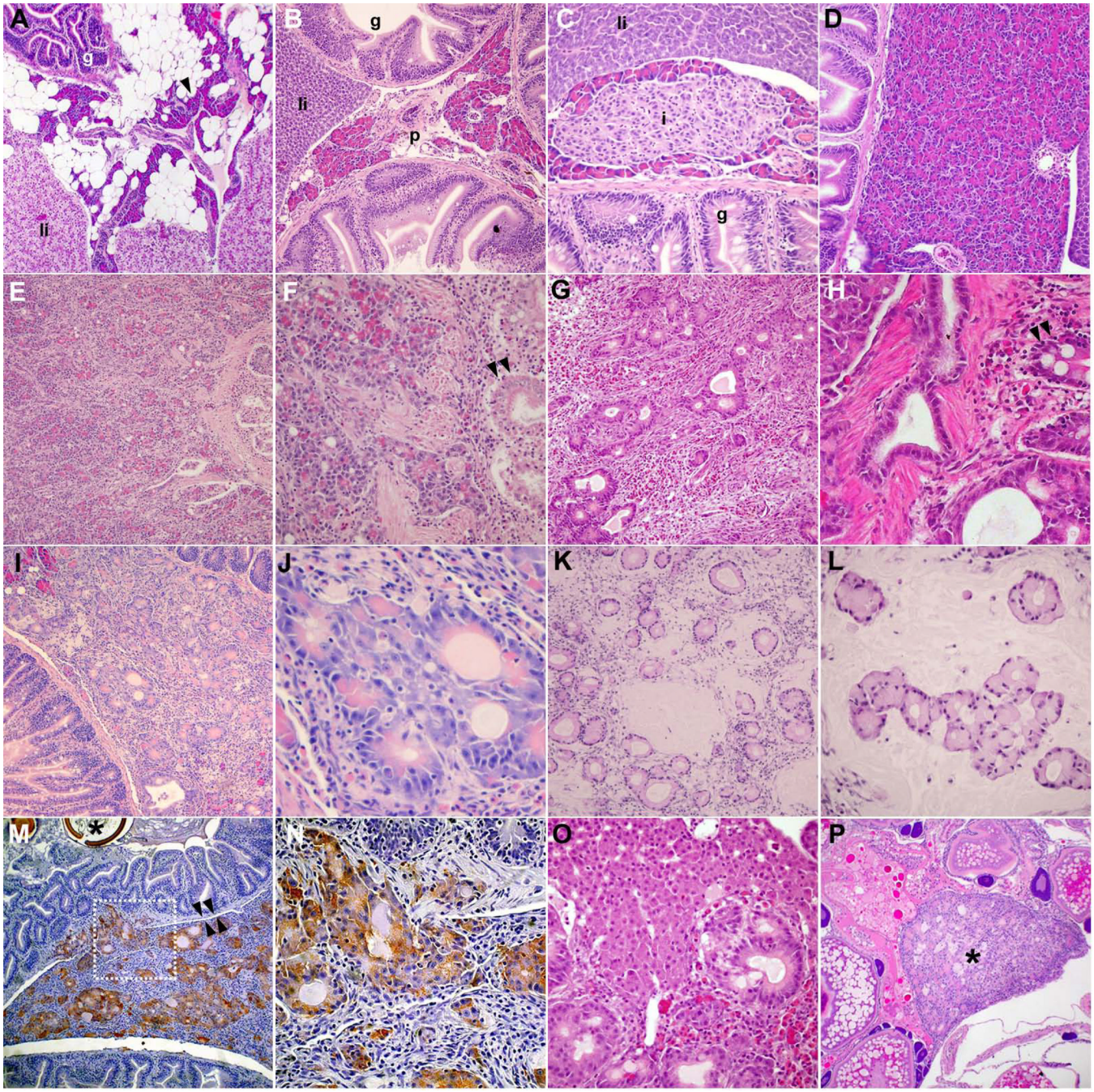

Fig. 5. Histological examination of normal adult zebrafish pancreas and *eGFP-KRAS*^{G12V}-induced pancreatic tumors

A–C, Normal pancreas in *ptf1a:eGFP* transgenics Arrowhead in (A) indicates pancreatic parenchyma surrounded by adipose tissue. D, increased size of exocrine pancreas (acinar hyperplasia) in Tg(*ptf1a:eGFP-KRAS*^{G12V}) fish with separate pancreatic tumor. E and F, Mixed adenocarcinoma with predominantly acinar cell differentiation and invasion of adjacent gut. Black arrowheads in F indicate base of intestinal crypt. G and H, Invasive adenocarcinoma with predominantly ductal differentiation and extensive desmoplastic reaction. Malignant glands are shown invading adjacent gut in H. Black arrowheads in H indicate base of intestinal crypt with adjacent goblet cells. I and J, adenocarcinoma with mixed acinar and glandular

features. K and L, mucinous (colloid) adenocarcinoma. Note tumor cells floating in abundant pools of extracellular mucin. M and N, immunohistochemical detection of eGFP-KRAS^{G12V} expression in invasive adenocarcinoma invading adjacent gut. Image in (N) represents magnified view of boxed area in (M). Black arrowheads in (M) indicate normal interface between pancreas and intestine. Asterisk in (M) indicates ingested brine shrimp egg in the gut lumen. O, invasion of adjacent liver by ductal adenocarcinoma. P, isolated tumor deposit (asterisk) in ovary. Abbreviations: g, gut; p, pancreas; li, liver. Magnification: A, and M, 100x; B, E, G, I, K, and P, 200x; C, D, F, H, J, L, N, and O, 400x.

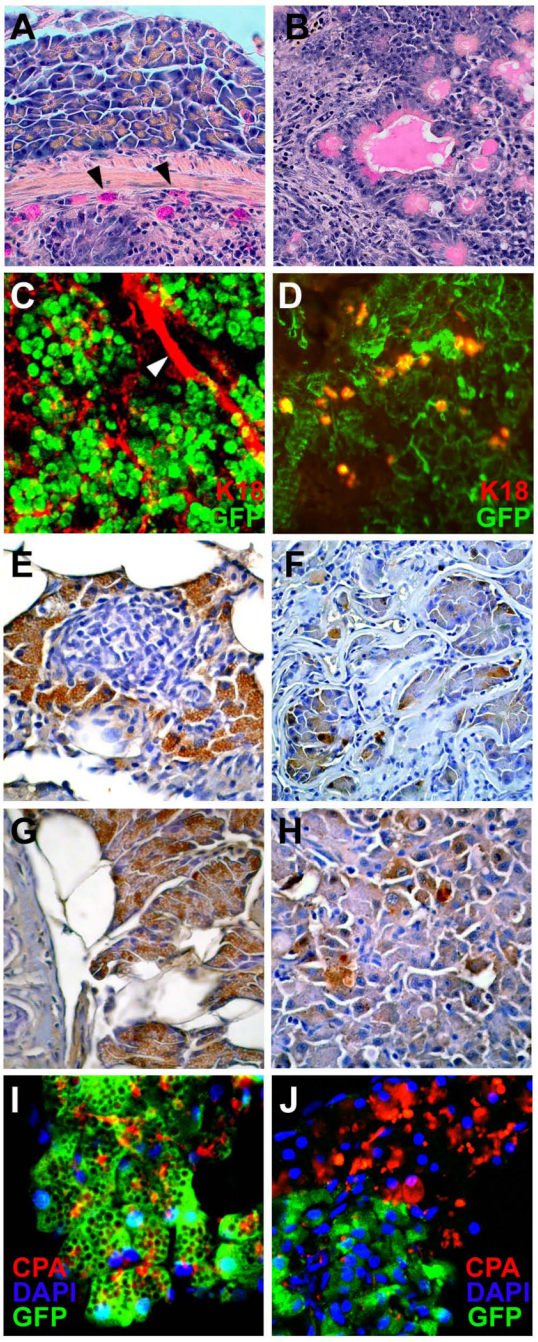

Fig. 6. Evaluation of differentiation and proliferation in normal adult zebrafish pancreas and *eGFP-KRAS*^{G12V}-induced pancreatic tumors

A, mucicarmine stain highlighting intracytoplasmic mucin in intestinal goblet cells, but not in adjacent normal pancreatic acinar cells (400x). B, Mucicarmine stain identifies intracytoplasmic and intralumenal mucin in a *eGFP-KRAS*^{G12V}-induced pancreatic tumor with ductal differentiation (400x). C and D (400x), immunofluorescent staining for Cytokeratin 18 reveals ductal elements in normal ptf1a:eGFP pancreas (C) and areas of ductal differentiation in *eGFP-KRAS*^{G12V}-induced pancreatic tumor (D). E and F (400x), immunohistochemical staining for amylase in normal pancreas (E) and *eGFP-KRAS*^{G12V}-induced pancreatic tumor (F). Normal pancreas demonstrates strong expression of amylase in exocrine acinar cells, but

not in endocrine islet (central area). Tumor in (F) shows acinar-like features, with some cells staining positive for amylase. G and H (400x), immunohistochemical staining for carboxypeptidase A (CPA) in normal pancreas (G) and *eGFP-KRAS*^{G12V}-induced pancreatic tumor (F). Normal pancreas shows strong CPA expression in exocrine acinar cells. Tumor in (H) shows acinar-like features, with some cells staining positive for CPA. I and J (400X), immunofluorescent labeling for CPA in combination with eGFP fluorescence. G, normal pancreas from Tg(*ptf1a:eGFP*) fish, showing widespread CPA expression in eGFP-positive acinar cells. H, Pancreatic tumors from Tg(*ptf1a:eGFP-KRAS*^{G12V}) fish, demonstrating that cells with high-level CPA expression are negative for the *ptf1a:eGFP-KRAS*^{G12V} transgene.

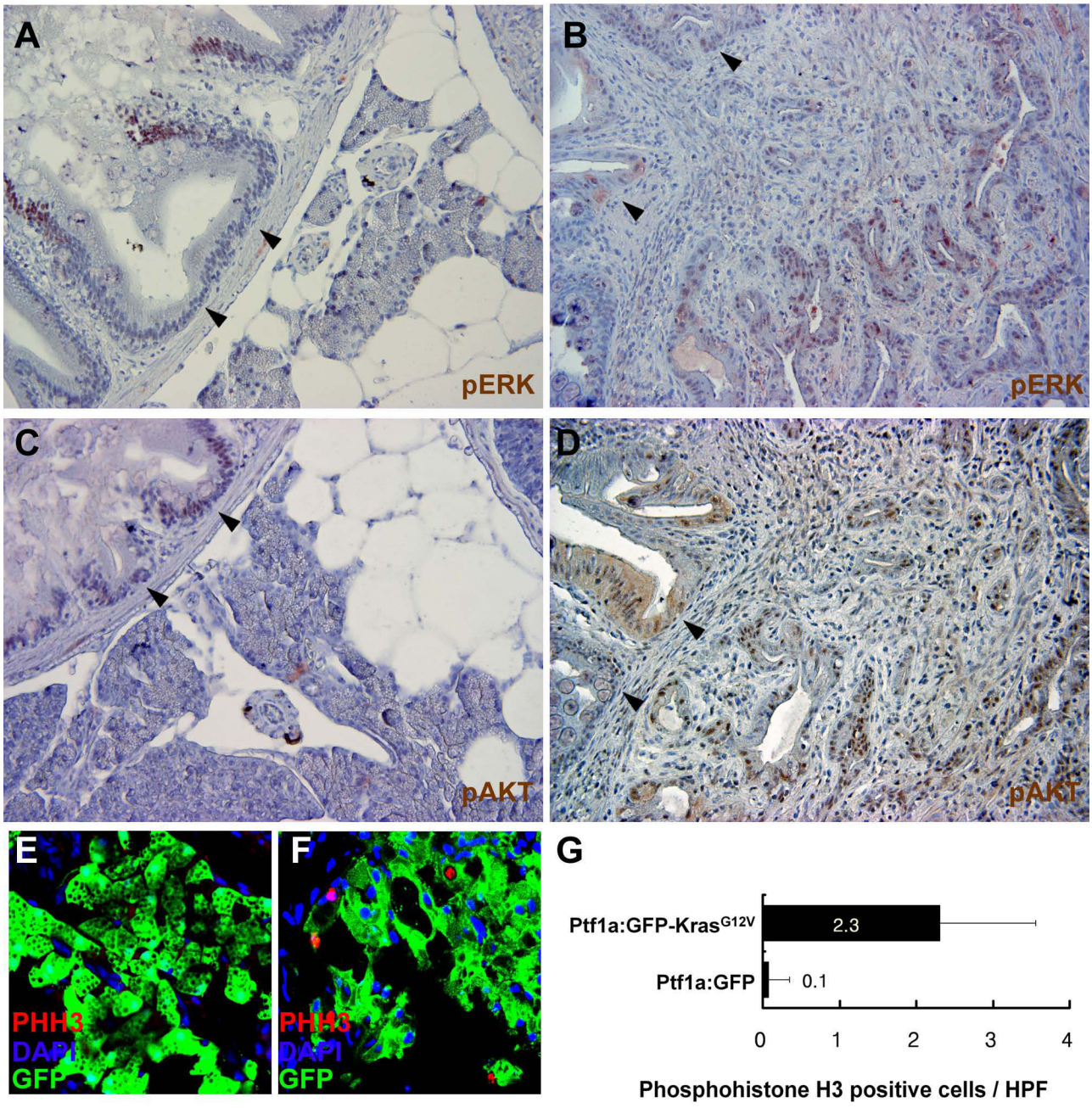

Fig. 7. Assessment of ERK and AKT signaling in eGFP-KRAS^{G12V}-induced pancreatic tumors

A and B (200x), immunohistochemical detection of phosphorylated ERK in normal zebrafish gut and pancreas (A), and in eGFP-KRAS^{G12V}-induced pancreatic tumor (B). C and D, immunohistochemical detection of phosphorylated AKT in normal zebrafish gut and pancreas (C), and in eGFP-KRAS^{G12V}-induced pancreatic tumor (D). Arrowheads in A–D indicate labeling in intestinal crypts. E and F (400x), immunofluorescent labeling for phospho-histone H3 (PHH3), a marker of proliferation, in normal pancreas from Tg(*ptf1a:eGFP*) fish (E), and pancreatic tumor from Tg(*ptf1a:eGFP-KRAS^{G12V}*) fish (F). G, Phosphohistone H3-positive cells per high power field (mean ± SEM).

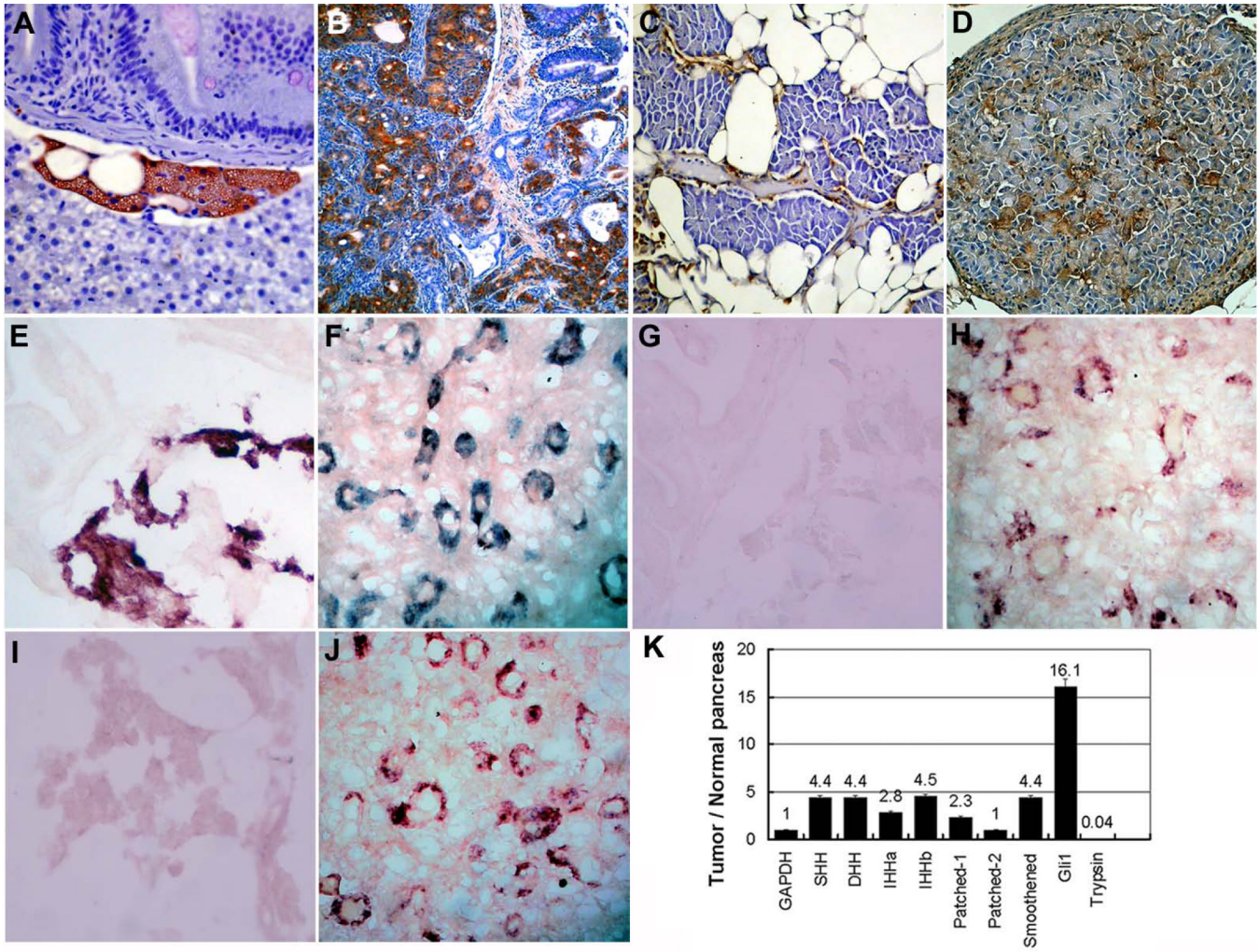

Fig. 8. Activation of hedgehog signaling pathway in eGFP-KRAS^{G12V}-induced pancreatic tumors

A and B, immunohistochemical stains for eGFP, showing transgene expression in exocrine pancreas of adult Tg(*ptf1a:eGFP*) fish (A, 400X) and in tumor from Tg(*ptf1a:eGFP-KRAS^{G12V}*) fish (B, 200X). C and D, immunohistochemical detection of Patched-2 in normal pancreas (C, 400X) and in *eGFP-KRAS^{G12V}*-induced pancreatic tumor (D, 200X). Patched-2 is expressed in tumor epithelium, but is confined to stromal elements in normal pancreas. E and F, in situ hybridization with *eGFP* probe detects *eGFP* expression in *ptf1a:eGFP* transgenic pancreas (E, 200X) and eGFP-KRAS^{G12V} expression in *ptf1a:eGFP-KRAS^{G12V}*-induced tumor (F, 200X). G and H, in situ hybridization for *smoothened* in normal pancreas (G, 200X) and in *eGFP-KRAS^{G12V}*-induced pancreatic tumor (H, 200X). *Smoothened* transcripts are detected in *eGFP-KRAS^{G12V}*-induced tumor, but not in normal pancreas. I and J, in situ hybridization for *gli1* in normal pancreas (I, 200X) and *eGFP-KRAS^{G12V}*-induced pancreatic tumor (J, 200X). Transcripts for *gli1* are detected in *eGFP-KRAS^{G12V}*-induced tumor, but not in normal pancreas. K, quantitative RT-PCR confirms upregulated expression of *sonic hedgehog*, *desert hedgehog*, *indian hedgehog a*, *indian hedgehog b*, *patched-1*, *smoothened* and *gli1*, and downregulated expression of *trypsin* in eGFP-KRAS^{G12V}–induced tumors relative to control pancreas. Values indicate mean ± SEM.

Table 1

Histopathologic findings in selectively sacrificed Tg(*ptf1a:GFP-KRAS^{G12V}*) fish

Note that in the absence of defined routes for tumor dessemination in fish, interpretation of metastatic disease is viewed as less than definitive.

Number	Age at sacrifice (months)	Transcutaneous fluorescence	Histology	Invasion & possible metastasis
1	2	None	No tumor	
2	2	None	No tumor	
3	4	None	No tumor	
4	4	Focal	Small tumor, acinar differentiation	
5	6	None	No tumor	
6	6	None	No tumor	
7	6	None	No tumor	
8	6	None	No tumor	
9	6	None	No tumor	
10	6	Focal	Small tumor, acinar differentiation	
11	6	Focal	Small tumor, acinar differentiation	
12	6	Focal	Small tumor, acinar differentiation, acinar hyperplasia	
13	6	Focal	Small tumor, acinar differentiation, acinar hyperplasia	
14	6	Diffuse	Large tumor, mixed acinar & ductal differentiation	
15	6	Diffuse	Mixed acinar & ductal differentiation	Liver & gut invasion, ovarian metastasis
16	6	Diffuse	Predominantly ductal differentiation	Gut invasion
17	8	None	No tumor	
18	8	None	No tumor	
19	8	None	No tumor	
20	8	None	No tumor	
21	8	None	No tumor, acinar hyperplasia	
22	8	None	Small tumor, acinar differentiation, acinar hyperplasia	
23	8	Focal	Small tumor, acinar differentiation, acinar hyperplasia	
24	8	Focal	Small tumor, ductal differentiation	
25	8	Focal	Small tumor, mixed acinar & ductal differentiation	
26	8	Diffuse	Mixed predominantly acinar differentiation	Invasion of muscle and ovary, spinal metastasis
27	8	Diffuse	Mixed acinar & ductal differentiation	Ovarian metastasis
28	8	Diffuse	Mixed acinar & ductal differentiation	Liver & gut invasion, ovarian metastasis
29	8	Diffuse	Mixed predominantly ductal differentiation	Liver & gut invasion

Number	Age at sacrifice (months)	Transcutaneous fluorescence	Histology	Invasion & possible metastasis
30	11	Diffuse	Ductal/mucinous differentiation	Liver and ovary invasion
31	11	Diffuse	Mixed predominantly ductal differentiation	Ovary invasion
32	11	Diffuse	Mixed predominantly acinar differentiation	Gut and liver invasion